The duration of mitosis and daughter cell size are modulated by nutrients in budding yeast

Ricardo M. Leitao and Douglas R. Kellogg

Department of Molecular, Cell and Developmental Biology, University of California, Santa Cruz, CA

The size of nearly all cells is modulated by nutrients. Thus, cells growing in poor nutrients can be nearly half the size of cells in rich nutrients. In budding yeast, cell size is thought to be controlled almost entirely by a mechanism that delays cell cycle entry until sufficient growth has occurred in G1 phase. Here, we show that most growth of a new daughter cell occurs in mitosis. When the rate of growth is slowed by poor nutrients, the duration of mitosis is increased, which suggests that cells compensate for slow growth in mitosis by increasing the duration of growth. The amount of growth required to complete mitosis is reduced in poor nutrients, leading to a large reduction in cell size. Together, these observations suggest that mechanisms that control the extent of growth in mitosis play a major role in cell size control in budding yeast.

Introduction

Cell growth during the cell cycle must be precisely controlled to ensure that cell division yields two viable cells of a defined size. This is achieved by cell size checkpoints, which delay key cell cycle transitions until an appropriate amount of growth has occurred. The mechanisms by which cell size checkpoints measure growth and trigger cell cycle transitions are poorly understood.

An interesting feature of cell size checkpoints is that they can be modulated by nutrients. Thus, in many kinds of cells, the amount of growth required to proceed through the cell cycle is reduced in poor nutrient conditions, which can lead to a nearly twofold reduction in size (Johnston et al., 1977; Young and Fantes, 1987). Nutrient modulation of cell size is likely an adaptive response that allows cells to maximize the number of cell divisions that can occur when nutrients are limited. Nutrient modulation of cell size is of interest because it likely works by modulating the threshold amount of growth required for cell cycle progression. Thus, discovering mechanisms of nutrient modulation of cell size should lead to broadly relevant insight into how cell size is controlled.

Cell size checkpoints are best understood in yeast, where two checkpoints have been defined. One operates at cell cycle entry in G1 phase, whereas the other operates at mitotic entry (Nurse, 1975; Johnston et al., 1977). The G1 phase checkpoint delays transcription of G1 cyclins, which is thought to be the critical event that marks commitment to enter the cell cycle (Cross, 1988; Nash et al., 1988). The mitotic entry checkpoint delays mitosis via the Wee1 kinase, which phosphorylates and inhibits mitotic Cdk1 (Nurse, 1975; Gould and Nurse, 1989).

In budding yeast, several lines of evidence suggest that cell size control occurs almost entirely at the G1 checkpoint. Budding yeast cell division is asymmetric, yielding a large mother cell and a small daughter cell. The small daughter cell spends more time undergoing growth in G1 before cell cycle entry (Johnston et al., 1977). This observation led to the initial idea of a G1 size checkpoint that blocks cell cycle entry until sufficient growth has occurred. The checkpoint is thought to control G1 cyclin transcription because loss of CLN3, the key early G1 cyclin that drives cell cycle entry, causes a delay in G1 phase (Cross, 1990). Cell growth continues during the delay, leading to abnormally large cells (Cross, 1988). Conversely, overexpression of CLN3 causes cell cycle entry at a reduced cell size (Cross, 1988; Nash et al., 1988). In contrast, loss of the Wee1 kinase, a key component of the mitotic checkpoint, causes only mild cell size defects in budding yeast (Jorgensen et al., 2002; Harvey and Kellogg, 2003; Harvey et al., 2005). Together, these observations suggest that cell size control occurs primarily during G1.

Although significant cell size control occurs in G1 phase, there is evidence that important size control occurs at other phases of the cell cycle in budding yeast. For example, cells lacking all known regulators of the G1 cell size checkpoint show robust nutrient modulation of cell size (Jorgensen et al., 2004). This could be explained by the existence of additional G1 cell size control mechanisms that have yet to be discovered, but it could also suggest that normal nutrient modulation of cell size requires checkpoints that work outside of G1 phase. More evidence comes from the observation that daughter cells complete mitosis at a significantly smaller size in poor nutrients than in rich nutrients (Johnston et al., 1977). This suggests the existence of a checkpoint that operates after G1, during bud growth, to control the size at which daughter cells are born. This possibility has not received significant attention because early work suggested that the duration of daughter bud growth

Correspondence to Douglas R. Kellogg: dkellogg@ucsc.edu



Downloaded from http://rupress.org/jcb/article-pdf/216/11/3463/1596705/jcb_201609114.pdf by guest on 02 December 2025

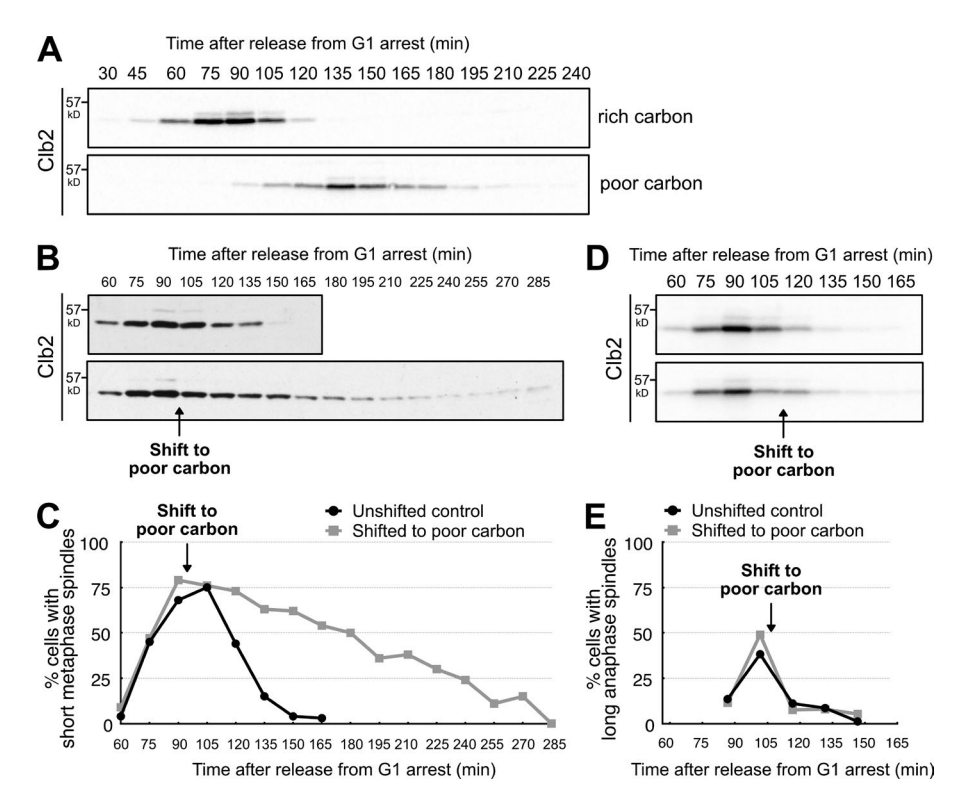


Figure 1. The duration of mitosis is modulated by nutrients. (A) Wild-type cells growing in YPD (rich carbon) or YPG/E (poor carbon) were arrested in G1 phase by addition of mating pheromone. The cells were released from arrest, and levels of mitotic cyclin Clb2 were assayed by Western blot. (B and C) Cells growing in YPD were released from G1 arrest. At 90 min, the culture was split, and one half was washed into YPD and the other half into YPG/E. Levels of mitotic cyclin Clb2 were assayed by Western blot (B), and cells with short metaphase spindles were assayed by immunofluorescence (C). (D and E) Cells growing in YPD were released from G1 arrest. At 105 min, the culture was split, and one half was washed into YPD and the other half into YPG/E. Levels of mitotic cyclin Clb2 were assayed by Western blot (D), and long anaphase spindles were assayed by immunofluorescence (E). Numbers on the left side of Western blots indicate molecular mass in kilodaltons.

is invariant and independent of nutrients (Hartwell and Unger, 1977). As a result, it has been thought that birth of small daughter cells in poor nutrients is a simple consequence of their reduced growth rate, rather than active size control. However, this has not been tested by directly measuring the duration of daughter cell growth in rich and poor nutrients, so it remains possible that checkpoints actively modulate the extent of daughter cell growth to control cell size at completion of mitosis.

Further evidence for size control outside of G1 phase has come from analysis of nutrient modulation of cell size. Protein phosphatase 2A associated with the Rts1 regulatory subunit (PP2A^{Rts1}) is required for nutrient modulation of cell size (Artiles et al., 2009). Proteome-wide analysis of proteins regulated by PP2A^{Rts1} revealed that it controls critical components of both the G1 phase and mitotic entry cell size checkpoints, as well as several key regulators of mitotic progression (Zapata et al., 2014). The fact that PP2A^{Rts1} is required for nutrient modulation of cell size, whereas regulators of the G1 checkpoint are not, could be explained by a model in which PP2A^{Rts1} controls mitotic cell size checkpoint mechanisms that play an important role in nutrient modulation of cell size.

Here, we set out to determine whether nutrient modulation of cell size occurs solely at the G1 checkpoint, or whether it also occurs at other times during the cell cycle. To do this, we investigated how nutrients affect cell growth, cell size, and cell cycle progression throughout the cell cycle.

Results and discussion

The duration of mitosis is modulated by nutrients

Previous work suggested that cell cycle events that occur after bud emergence have a constant duration that is independent of the growth rate set by nutrients (Hartwell and Unger, 1977). However, the limited tools available at the time meant that the duration of cell cycle events had to be inferred from indirect measurements. To more directly address this question, we first grew cells in a rich carbon source (2% dextrose) or a poor carbon source (2% glycerol + 2% ethanol) and determined the duration of mitosis by assaying levels of the mitotic cyclin Clb2 in synchronized cells. Clb2 persisted for a longer interval in cells growing in poor nutrients, which suggested that the duration of mitosis is increased (Fig. 1 A).

We next asked whether cells already in mitosis were sensitive to a shift from rich to poor carbon. Cells growing in rich carbon were synchronized and shifted to poor carbon when Clb2 reached peak levels, and most cells had short mitotic spindles, indicating that they were in metaphase. A shift to poor carbon at this point in mitosis caused a prolonged metaphase delay, as well as delayed destruction of Clb2 (Fig. 1, B and C). In contrast, if cells were switched to poor carbon slightly later in mitosis, when cells were in anaphase, there was no delay in destruction of Clb2 or completion of anaphase (Fig. 1, D and E). The insensitivity of anaphase cells to carbon source suggests that the metaphase delay is not due simply to a starvation response, which would likely affect both metaphase and anaphase.

To further investigate the effects of nutrients, we used fluorescence and bright-field microscopy to simultaneously monitor daughter bud growth and mitotic events in living cells. Bud growth was monitored by plotting daughter bud volume as a function of time. To monitor key events of mitosis, mitotic spindle poles were marked with Spc42-GFP, and the distance between poles was plotted as a function of time. Initiation of metaphase corresponds to the initial separation of spindle poles, whereas the duration of metaphase corresponds to the interval when spindle poles remain separated by 1–2 µm within the mother cell (Winey and O'Toole, 2001; Lianga et al., 2013). Initiation of anaphase is detected when spindle poles begin to move further apart and one pole migrates into

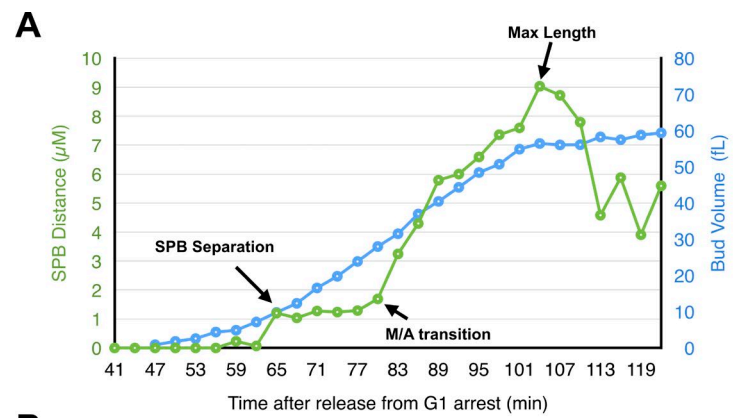
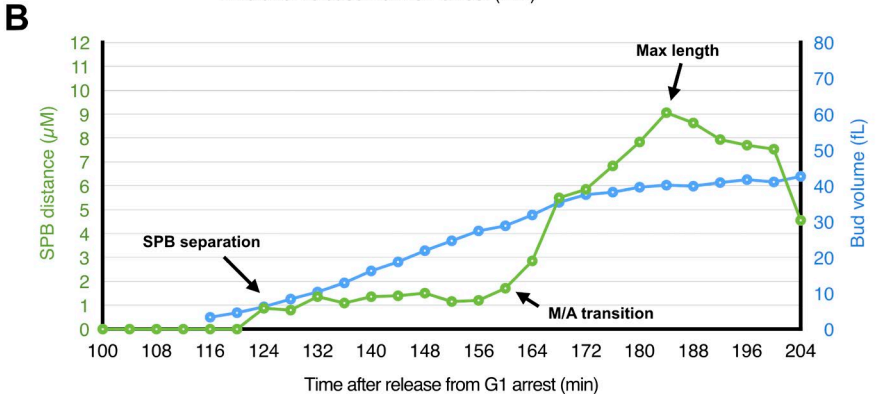
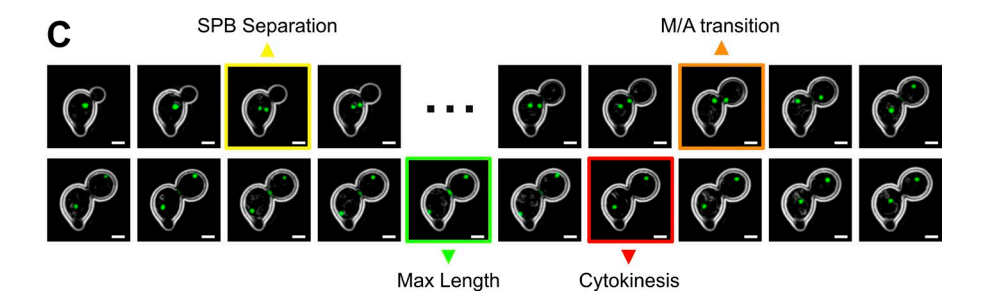


Figure 2. Simultaneous imaging of bud growth and mitotic spindle dynamics. (A and B) Representative growth curves for cells growing in rich carbon (A) or poor carbon (B). The volume of the daughter bud is plotted in blue, and the distance between spindle poles in green. (C) Contrast-enhanced images of a representative growing bud with GFP-tagged spindle poles (Spc42-GFP) and myosin ring (Myo1-GFP). Key transitions are highlighted. "..." indicates images taken in metaphase that were omitted so that all key transition points could be shown. Bars, 2 μM.





the daughter cell. We defined the duration of anaphase as the interval between anaphase initiation and the time when the spindle poles reached their maximum distance apart. GFP-tagged myosin was used to detect completion of cytokinesis, which is marked by disappearance of the myosin ring (Lippincott and Li, 1998). In addition to the stages of mitosis, we defined an S/G2 interval as the time from bud emergence to spindle pole separation, and G1 phase as the time from when the daughter cell completes cytokinesis to when it initiates formation of a new daughter bud.

Bud growth and size were analyzed through a complete bud growth cycle, from the time the bud emerged from the mother cell to the time that it initiated formation of a new bud at the end of the next G1 phase. We used cells synchronized in G1 phase by mating pheromone arrest and release, as well as asynchronous cells. Cells synchronized by mating pheromone undergo growth during the arrest, and therefore initiate bud growth at a larger mother cell size than asynchronous cells (Fig. S1). For both synchronous and asynchronous cells, there was not a statistically significant difference between mean mother cell size in rich versus poor carbon. This indicates that any differences in daughter cell growth or cell cycle timing

between the two conditions are unlikely to be caused by differences in mother cell size.

Representative data for synchronous cells growing in rich and poor carbon are shown in Fig. 2 (A and B), respectively. Examples of cell images taken during the course of bud growth are shown in Fig. 2 C. At least 25 cells were analyzed under each condition (Fig. S2 [A and B] shows individual growth curves).

The durations of all cell cycle stages comprising a complete bud growth cycle in rich and poor carbon are shown in Fig. 3 A for synchronous cells and Fig. 3 B for asynchronous cells (Fig. S3 A shows scatter plots and p-values). To focus on the effects of carbon source on mitosis, we also plotted separately the mean durations of metaphase and anaphase for cells growing in rich or poor carbon (Fig. 3, C and D).

The durations of both metaphase and anaphase were significantly increased in poor carbon. The overall mean duration of mitosis was similar in the synchronous and asynchronous cells, although the fraction of mitosis spent in metaphase was slightly increased in asynchronous cells. The fraction of the growth cycle spent in G1 phase increased in poor carbon, as previously reported (Hartwell and Unger, 1977). The increase in G1 phase was greatest in asynchronous cells.

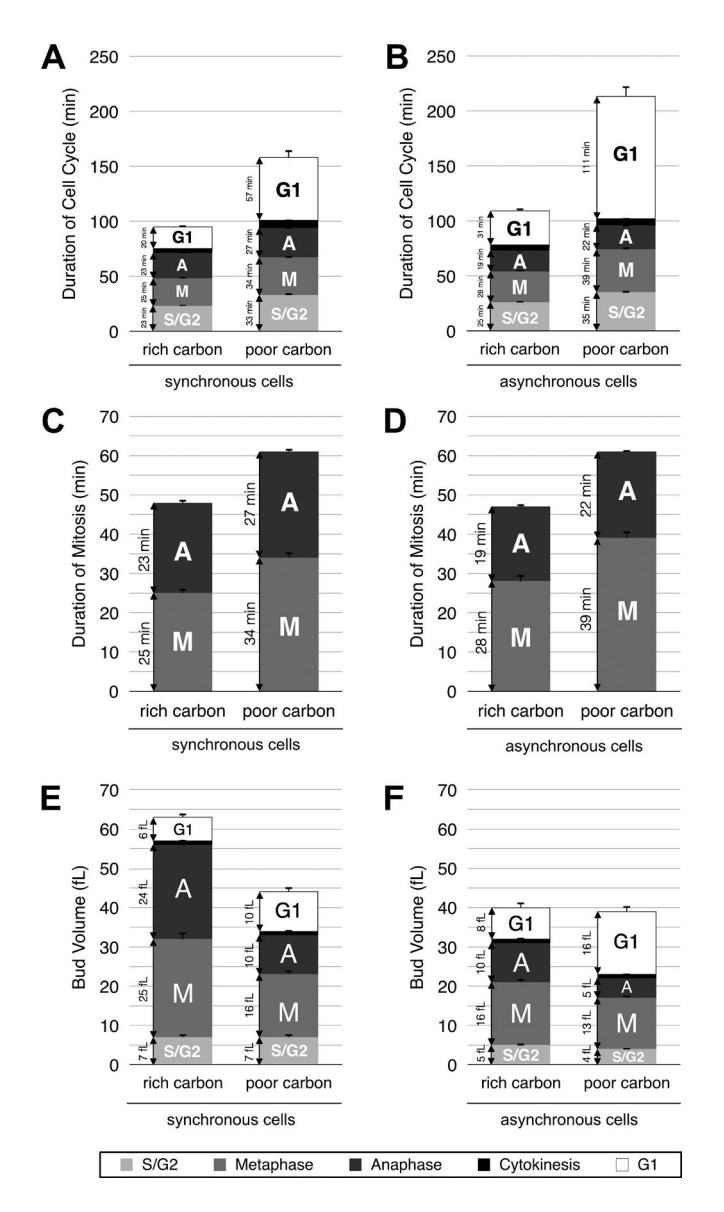


Figure 3. The duration of mitosis and cell size at completion of mitosis are modulated by nutrients. (A and B) Plots showing the mean durations of all cell cycle stages for synchronous cells (A) or asynchronous cells (B) growing in rich or poor carbon. (C and D) Plots showing the mean durations of metaphase and anaphase for synchronous cells (C) or asynchronous cells (D) growing in rich or poor carbon. (E and F) Plots showing the mean growth in volume during all phases of the cell cycle for synchronous cells (E) or asynchronous cells (F) growing in rich or poor carbon. Error bars represent SEM.

Daughter cell size is modulated by nutrients

We next plotted bud size at completion of each cell cycle stage (Fig. 3, E and F; and Fig. S3 B shows scatter plots and p-values). Cells in poor carbon completed each stage of mitosis at a significantly smaller size. The data also show that in both rich and poor carbon, more growth in volume occurs during mitosis than in G1 phase. The increased size of daughter cells in synchronous cells relative to asynchronous cells is consistent with previous studies that mother cell size influences daughter cell size (Johnston et al., 1977; Schmoller et al., 2015).

The data are inconsistent with a model in which cells complete mitosis at a reduced size in poor nutrients simply because their growth rate is reduced, whereas the duration of mitotic events is unchanged. Rather, the duration of mitosis and cell size at completion of mitosis are modulated in response to changes in carbon source that cause large changes in growth rate. The data therefore suggest the existence of a nutrient-modulated mechanism that measures growth during mitosis and delays completion of mitosis until sufficient growth has occurred. This would explain why cells shifted from rich to poor carbon during metaphase undergo a prolonged mitotic delay, whereas cells shifted during anaphase do not (Fig. 1, B-E). If the delay were a consequence of a reduction in ATP or other metabolites needed for mitotic spindle events, one would expect to see delays in both metaphase and anaphase. Rather, we suggest that a shift to poor carbon during metaphase causes a delay because the daughter bud has not yet undergone sufficient growth, whereas a shift in anaphase does not cause a delay because buds have already reached the threshold amount of growth needed to complete mitosis in poor carbon. Because a large fraction of total growth occurs in mitosis, it would make sense that mechanisms that control the extent of growth in mitosis play a significant role in cell size control. The existence of major cell size control mechanisms in mitosis would explain why cells lacking critical regulators of the G1 size checkpoint still show robust nutrient modulation of cell size (Jorgensen et al., 2004). Work in fission yeast has suggested that there are mitotic cell size control mechanisms that act independently of Cdk1 inhibitory phosphorylation, which could explain why loss of Cdk1 inhibitory phosphorylation in budding yeast causes only modest effects on cell size (Wood and Nurse, 2013).

An alternative model is that the duration of mitosis is controlled by a nutrient-modulated timer. In rich medium, the timer would be set for a short duration of growth, whereas in poor medium it would be set for a longer interval. However, comparison of the data from synchronous and asynchronous cells would appear to rule out a nutrient-modulated timer model. Synchronous cells spend a total of 51 min in metaphase and anaphase in poor carbon, whereas asynchronous cells spend 61 min, despite growing under identical nutrient conditions. The difference is most likely a result of slower growth rates in asynchronous cells (see Figs. 4 and 5), which would result in the need for a longer interval of growth to reach a critical amount of growth required for completion of mitosis. A timer model is also not consistent with the large variance in mitotic duration observed between individual cells growing under identical conditions (Fig. S3 A).

In both synchronous and asynchronous cells, the mean size of mother cells initiating bud emergence was only slightly smaller in poor carbon compared with rich carbon, and the difference was not statistically significant (Fig. S1). In addition, asynchronous daughter cells completed G1 phase at nearly identical sizes in rich and poor carbon (Fig. 3 F). These observations agree well with a previous study that found that cells growing in poor carbon complete late G1 phase at ~90\% of the size of cells in rich carbon (Di Talia et al., 2007). This may at first seem paradoxical, because poor carbon reduces mean size nearly twofold. However, cells in poor carbon grow slowly in mitosis, complete mitosis at a reduced cell size, and spend more time in G1 phase. As a result, they spend more time at small sizes compared with cells in rich carbon, which contributes to a smaller mean size when population averages are measured with a Coulter counter.

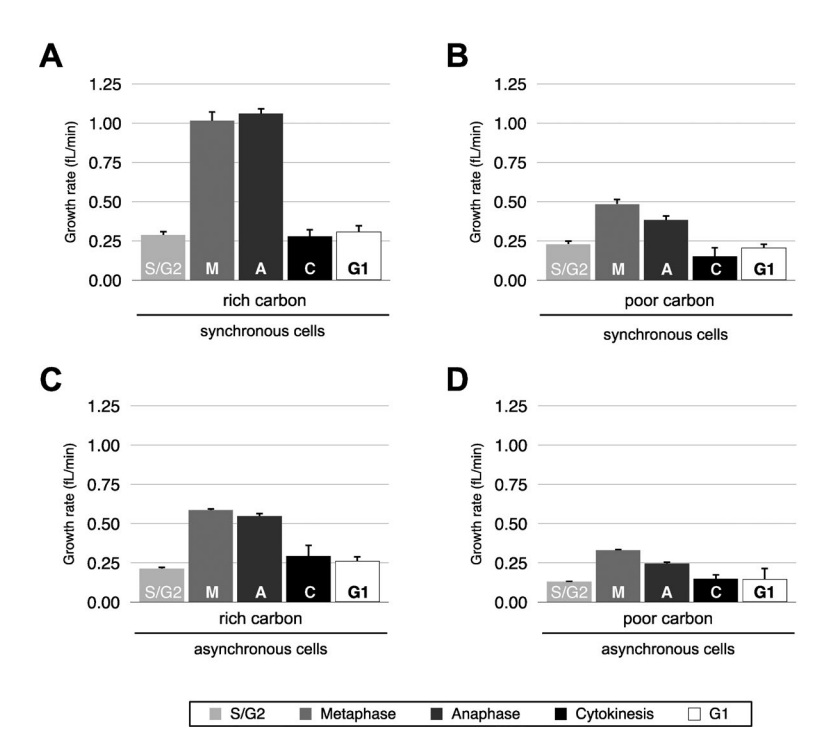


Figure 4. Cell growth rate is modulated during the cell cycle. The growth rate at each phase of the cell cycle was calculated as the mean of individual cell growth rates. Growth rate was calculated by dividing the volume increase of the cell during a phase by the time the cell spent in that phase. (A and B) Data for synchronous cells growing in rich carbon (A) or poor carbon (B). (C and D) Data for asynchronous cells growing in rich carbon (C) or poor carbon (D). Error bars represent SEM.

The rate of growth is modulated during the cell cycle

Previous studies suggested that growth rate changes during the cell cycle, but did not include analysis of growth during specific stages of mitosis in unperturbed single cells (Goranov et al., 2009; Ferrezuelo et al., 2012). To extend these studies, we calculated mean growth rates at each stage of the cell cycle in rich and poor carbon (Fig. 4, A and B, synchronous cells; and Fig. 4, C and D, asynchronous cells). When the bud first emerges, growth is relatively slow. Entry into mitosis initiates a fast growing phase that lasts nearly the entire length of mitosis. As cells complete anaphase, the growth rate slows. A slow rate of growth persists during G1 phase. Poor carbon reduced the rate of growth in mitosis by half but caused smaller reductions in growth rate during other stages of the growth cycle. The rate of bud growth was greater in synchronized cells, most likely because of increased mother cell size (Schmoller et al., 2015). Previous studies have shown that polar bud growth is driven by Cdk1 activity; however, the signals that control bud growth at other stages of the cell cycle are unknown (McCusker et al., 2007). Moreover, the mechanisms and function of growth rate modulation during the cell cycle are unknown.

The discovery that most growth in volume occurs during a rapid growth phase in mitosis provides more evidence that cell size homeostasis requires tight control over the interval of mitotic growth. For example, a 20% change in the duration of growth in mitosis would have a large effect on cell size, whereas a 20% change in the duration of growth in G1 phase would have a smaller effect because the rate of growth in G1 phase is substantially slower.

Effects of carbon source on daughter cell size are stronger than effects of mother cell size

Differences in cell growth and size between synchronous and asynchronous cells point to a strong influence of mother cell size on growth rate and daughter cell size. For example, synchronized cells initiate bud growth at a larger mother cell size compared with unsynchronized cells, and their daughter buds grow faster and complete mitosis at a larger size (Figs. 3, 4, and S1). Previous studies observed a similar correlation between mother cell size and daughter cell size (Johnston et al., 1977; Schmoller et al., 2015). These observations raised the possibility that the difference in daughter cell size at completion of mitosis in rich and poor carbon could be caused by differences in mother cell size as a result of nutrient modulation of cell size in G1 phase.

To further analyze the effects of mother cell size, we plotted the relationship between mother cell size and growth rate of the daughter bud in mitosis. Growth rate was positively correlated with mother cell size in both rich and poor carbon (Fig. 5, A and B, synchronous and asynchronous cells, respectively). Thus, daughters of large mothers grew faster than daughters of small mothers, consistent with the idea that mother cell size influences biosynthetic capacity. However, carbon source had a stronger influence on growth rate than mother cell size. This can be seen by the fact that mothers of similar size in rich and poor carbon had daughter buds that grew at different rates, which was true across the entire range of mother cell sizes.

We also plotted daughter cell size at completion of cytokinesis versus mother cell size (Fig. 5, C and D). Daughter cell size was positively correlated with mother cell size in both conditions. However, the influence of carbon source was again much stronger. Mother cells growing in poor carbon that were the same size as mother cells in rich carbon consistently produced much smaller daughter cells. Together, these data indicate that effects of carbon source on daughter cell size cannot be due solely to differences in mother cell size.

The effects of mother cell size could explain why synchronized cells in rich carbon completed late G1 phase at a larger size than their counterparts in poor carbon (Fig. 3 E). Note that synchronized cells in both rich and poor carbon appear to overshoot the size at which asynchronous cells complete late G1 phase, which could be caused by increased mother cell

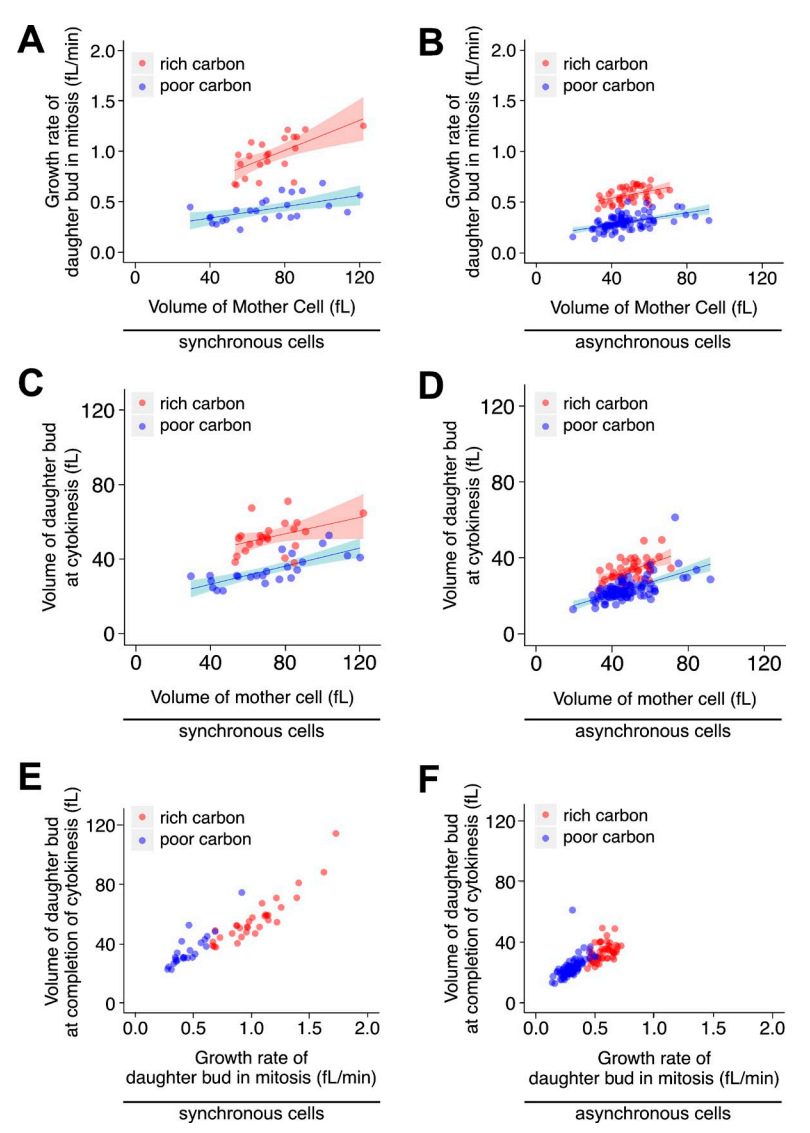


Figure 5. Cell size at completion of cytokinesis is proportional to growth rate during mitosis. (A and B) The growth rate in mitosis of each daughter bud was plotted against the volume of its mother cell for synchronous cells (A) and asynchronous cells (B). (C and D) The volume of each daughter bud at cytokinesis was plotted against the size of its mother for synchronous cells (C) and asynchronous cells (D). (E and F) The volume of daughter cells at cytokinesis was plotted against their growth rate during mitosis for synchronous cells (E) and asynchronous cells (F). Red dots, cells in rich carbon; blue dots, cells in poor carbon. Smooth lines are logistic regressions of the data. Shaded areas represent 95% confidence interval.

size in the synchronized cells. The large mothers in synchronized cells in rich carbon drive a high rate of growth, which could lead to greater overshooting of the threshold amount of growth required for G1 progression. Asynchronous cells in both rich and poor carbon have smaller mother cells and are born at smaller sizes relative to synchronized cells. In this case, compensatory growth in G1 appears to become more important to bring the daughter cell up to a minimal threshold size before cell cycle entry.

Cell size at completion of mitosis is correlated with growth rate during mitosis. Previous studies found that cell size at the end of G1 phase is correlated with growth rate during G1 phase (Johnston et al., 1979; Ferrezuelo et al., 2012). The correlation holds true when comparing cells growing in the same carbon source and when comparing cells growing in different carbon sources. To determine whether a similar relationship exists for growth during mitosis, we plotted daughter cell size at cytokinesis as a function of daughter bud growth rate during mitosis for cells growing in rich or poor carbon (Fig. 5, E and F). Daughter cell size was positively correlated with growth rate under both conditions. Thus, cell size at all key cell cycle transitions is correlated with growth rate.

Because cell size is proportional to growth rate, faster growing cells should always give rise to larger daughter cells. Moreover, because growth rate is proportional to size, larger mother cells should have a higher growth rate, leading to ever larger daughter cells. In this case, what limits cell size? The plot of daughter bud size at cytokinesis as a function of mother cell size revealed that daughter cell size indeed increases with mother cell size, but the ratio of mother size to daughter size is not constant across the range of mother cell sizes (Fig. 5, C and D). In other words, small mothers produce daughters of nearly equal size, whereas very large mothers produce daughters that are nearly half the size of the mother (Johnston et al., 1977). This relationship would correct large variations in mother cell size, which could be the result of growth during cell cycle delays induced by other checkpoints, such as the spindle checkpoint or DNA damage checkpoints.

The strong correlation between growth rate and cell size is difficult to reconcile with simple cell size checkpoint models in which a threshold volume must be reached to pass the checkpoint. If a specific volume must be reached to pass a checkpoint, the rate at which the cell reaches that volume should not influence the final volume at which the cell passes the checkpoint. One way to reconcile the idea of a set threshold volume

with growth rate dependence would be to imagine that cell size checkpoint thresholds are noisy and imperfect. In this view, faster growing cells will overshoot the threshold size more than slow growing cells, leading to increased size. However, this model would not explain nutrient modulation of cell size. Thus, another model could be that cells measure their growth rate and set cell size thresholds to match growth rate (Jorgensen et al., 2004). Alternatively, the same signals that set the growth rate could also set the cell size threshold. Because nutrients modulate growth rate, both models would explain nutrient modulation of cell size.

Materials and methods

Yeast strains and media

The genotype of the strain used in this study is SPC42-GFP::HIS3 MYO1-GFP::TRP1 leu2-3,112 ura3-1 can1-100 ade2-1 his3-11,15 trp1-1 GAL+, ssd1-d2 (W303 background). Genetic alterations were performed using one-step PCR-based integration at the endogenous locus (Longtine et al., 1998) or by genetic crossing.

For cell cycle time courses, cells were grown in YP medium (1% yeast extract, 2% peptone, and 40 μ g/ml adenine) supplemented with 2% dextrose (YPD) or 2% glycerol and 2% ethanol (YPG/E). For microscopy, cells were grown in complete synthetic medium (CSM) supplemented with 2% dextrose (CSM-Dex) or 2% glycerol and 2% ethanol (CSM-G/E).

Microscopy

Cells were grown overnight in CSM-DEX or CSM-G/E at room temperature with constant rotation to an optical density near 0.1 at λ 600. 5 ml of culture was arrested with α factor at 0.5 μg/ml for 3–4 h. Cells were released from the arrest by three consecutive washes with the same medium and resuspended in 500 µl medium. Approximately 200 µl of cell suspension was spotted on a concanavalin A-treated glass-bottom dish with a 10-mm microwell #1.5 cover glass. Cells were adhered for 5 min, and unbound cells were washed away by repeated washing with 1 ml prewarmed medium. The dish was then flooded with 3 ml medium and placed on a temperature-controlled microscope stage set to 27°C (Pecon Tempcontrol 37-2 digital). The temperature of the medium was monitored throughout the experiment using a MicroTemp TQ1 reader coupled to a Teflon insulated K-type thermocouple (Omega). The probe was placed in contact with the glass bottom near the contact area between the objective and the dish. Temperature was maintained at 27 ± 1°C; imaging sessions in which the temperature varied beyond this limit were rejected from final analysis. Bright-field and fluorescent images were acquired simultaneously using an LSM 5 Pascal Axiovert 200M inverted microscope (Zeiss) and a Plan-Apochromat 63×/1.4 oil objective. 488-nm light was obtained from an argon laser light source using a (488/543/633) primary dichroic beam splitter (HFT). The laser was set to 0.7% intensity. For green fluorescence images, light was collected through a longpass 505 emission filter using a 1-AU size pinhole. Bright-field images were collected using the transmitted light detector. Optical sections were taken for a total of 11 z-planes every 0.5 µm with frame averaging set to 2, to reduce noise. The total exposure was kept as low as possible to limit photo damage (1.60-us dwell time per pixel, image dimension set to 512×512 pixels, and pixel size set to 0.14×0.14 µm). Images were acquired at 3-min intervals for rich carbon and 4-min intervals for poor carbon and recorded via the Zen 2000 interface.

Image analysis

Image analysis was performed using ImageJ (Linkert et al., 2010; Schneider et al., 2012). The ImageJ plug-ins StackReg and MultiStackReg were used for postacquisition image stabilization (Thévenaz et al., 1998). Stabilized bright-field images were processed using the ImageJ plug-in FindFocusedSlices, and the volume of growing buds was determined using BudJ (Ferrezuelo et al., 2012). Bud volumes were measured for buds whose focal plane was no more than 1.5-um away (three z-steps) from the mother cell's focal plane. Sum projections of z-stacks were treated using a 2-pixel mean filter, and brightness/contrast levels were adjusted to reduce background noise. The treated pseudo-colored green fluorescent images were overlapped with the outlines of the imaged cells for reference (outlines were generated using the "find edges" command over a sum projection of all z-stacks of bright field images). Positions of spindle poles were determined using the crosshair tool (set to auto-measure and auto-next), and distance between the two spindle poles was determined using the mathematical formula for the distance between two points. Disappearance of the Myo1 ring was determined empirically by observation of GFP signal at the bud neck.

Statistical analysis

Data acquired from ImageJ was analyzed using Apple Numbers, R (R Core Team, 2016), RStudio (RStudio Team, 2015), and the R package ggplot2 (Wickham, 2009). P-values were calculated using a Welch two-sample *t* test and a 95% confidence interval.

Cell cycle time courses and Western blotting

For Western blot time courses, cells were grown overnight at room temperature in liquid YPD or YPG/E to an optical density of 0.5 at λ 600. Because optical density is affected by cell size, we normalized cell numbers by counting cells with a Coulter counter (Beckman Coulter) when comparing cells grown in rich and poor carbon.

G1 synchronization was achieved by arresting cells with α factor at a concentration of 0.5 µg/ml until at least 90% of cells were unbudded. Cells were released from arrest by washing three times with fresh medium. Time courses were performed at 25°C with constant agitation. To prevent cells from reentering the next cell cycle, α factor was added back after most cells had budded. For nutrient shift time courses, a single culture was arrested and split at the moment of release from G1 arrest. At the time of the shift, both cultures were washed three times with room temperature YPD (control) or YPG/E (shifted cells) by centrifugation for 1 min at 3,000 g (Eppendorf 5702). The volume of the culture was restored to its original volume before the washes and cultures were placed back at 25°C.

For Western blots, 1.6-ml samples were collected at regular intervals, pelleted, and flash frozen in presence of 200 μ l glass beads. Cell lysis and Western blotting were performed as previously described (Harvey et al., 2005).

Immunofluorescence analysis of mitotic spindles was performed as previously described (Pringle et al., 1991). Multiplane imaging of slides was performed using a Leica DM5500 B Widefield Microscope and a 63×/0.6–1.4 oil objective. Spindles were counted in ImageJ. Data were processed and plotted using Apple Numbers.

Online supplemental material

Fig. S1 shows distributions of mother cell volumes for cells growing in rich or poor carbon and for synchronous and asynchronous cultures. Fig. S2 shows growth curve data for cells growing in rich or poor carbon. Fig. S3 shows dot plot versions of the data used to generate Fig. 3.

Acknowledgments

We thank Ben Abrams, Facilities Manager for the UCSC Life Sciences Microscopy Center, for support and mentoring with all microscopy-related techniques, and the Aldea laboratory for sharing BudJ, an ImageJ plugin to analyze images of budding yeast cells.

R. Leitao was supported by a fellowship from the Fundação para a Ciência e a Tecnologia, with funds from Programa Operacional Potencial Humano/Fundo Social Europeu, under the fellowship SFRH/BD/75004/2010. This work was supported by National Institutes of Health grant R01-GM053959.

The authors declare no competing financial interests.

Author contributions: R. Leitao contributed conceptualization, investigation, data curation, formal analysis, methodology, software, visualization, writing, review, and editing. D. Kellogg contributed conceptualization, methodology, writing, review, editing, supervision, project administration, and funding acquisition.

Submitted: 25 September 2016 Revised: 11 June 2017 Accepted: 23 August 2017

References

- Artiles, K., S.D. Anastasia, D. McCusker, and D.R. Kellogg. 2009. The Rts1 regulatory subunit of protein phosphatase 2A is required for control of G1 cyclin transcription and nutrient modulation of cell size. *PLoS Genet*. 5:e1000727. http://dx.doi.org/10.1371/journal.pgen.1000727
- Cross, F.R. 1988. DAF1, a mutant gene affecting size control, pheromone arrest, and cell cycle kinetics of Saccharomyces cerevisiae. *Mol. Cell. Biol.* 8:4675–4684. http://dx.doi.org/10.1128/MCB.8.11.4675
- Cross, F.R. 1990. Cell cycle arrest caused by CLN gene deficiency in Saccharomyces cerevisiae resembles START-I arrest and is independent of the mating-pheromone signalling pathway. *Mol. Cell. Biol.* 10:6482–6490. http://dx.doi.org/10.1128/MCB.10.12.6482
- Di Talia, S., J.M. Skotheim, J.M. Bean, E.D. Siggia, and F.R. Cross. 2007. The effects of molecular noise and size control on variability in the budding yeast cell cycle. *Nature*. 448:947–951. http://dx.doi.org/10.1038/nature06072
- Ferrezuelo, F., N. Colomina, A. Palmisano, E. Garí, C. Gallego, A. Csikász-Nagy, and M. Aldea. 2012. The critical size is set at a single-cell level by growth rate to attain homeostasis and adaptation. *Nat. Commun.* 3:1012. http://dx.doi.org/10.1038/ncomms2015
- Goranov, A.I., M. Cook, M. Ricicova, G. Ben-Ari, C. Gonzalez, C. Hansen, M. Tyers, and A. Amon. 2009. The rate of cell growth is governed by cell cycle stage. *Genes Dev.* 23:1408–1422. http://dx.doi.org/10.1101/gad .1777309
- Gould, K.L., and P. Nurse. 1989. Tyrosine phosphorylation of the fission yeast cdc2+ protein kinase regulates entry into mitosis. *Nature*. 342:39–45. http://dx.doi.org/10.1038/342039a0
- Hartwell, L.H., and M.W. Unger. 1977. Unequal division in Saccharomyces cerevisiae and its implications for the control of cell division. J. Cell Biol. 75:422–435. http://dx.doi.org/10.1083/jcb.75.2.422
- Harvey, S.L., and D.R. Kellogg. 2003. Conservation of mechanisms controlling entry into mitosis: Budding yeast weel delays entry into mitosis and is required for cell size control. *Curr. Biol.* 13:264–275. http://dx.doi.org/10 .1016/S0960-9822(03)00049-6
- Harvey, S.L., A. Charlet, W. Haas, S.P. Gygi, and D.R. Kellogg. 2005. Cdk1-dependent regulation of the mitotic inhibitor Wee1. Cell. 122:407–420. http://dx.doi.org/10.1016/j.cell.2005.05.029

- Johnston, G.C., J.R. Pringle, and L.H. Hartwell. 1977. Coordination of growth with cell division in the yeast Saccharomyces cerevisiae. Exp. Cell Res. 105:79–98. http://dx.doi.org/10.1016/0014-4827(77)90154-9
- Johnston, G.C., C.W. Ehrhardt, A. Lorincz, and B.L.A. Carter. 1979. Regulation of cell size in the yeast Saccharomyces cerevisiae. J. Bacteriol. 137:1–5.
- Jorgensen, P., J.L. Nishikawa, B.J. Breitkreutz, and M. Tyers. 2002. Systematic identification of pathways that couple cell growth and division in yeast. *Science*. 297:395–400. http://dx.doi.org/10.1126/science.1070850
- Jorgensen, P., I. Rupes, J.R. Sharom, L. Schneper, J.R. Broach, and M. Tyers. 2004. A dynamic transcriptional network communicates growth potential to ribosome synthesis and critical cell size. *Genes Dev.* 18:2491–2505. http://dx.doi.org/10.1101/gad.1228804
- Lianga, N., E.C. Williams, E.K. Kennedy, C. Doré, S. Pilon, S.L. Girard, J.-S. Deneault, and A.D. Rudner. 2013. A Wee1 checkpoint inhibits anaphase onset. J. Cell Biol. 201:843–862. http://dx.doi.org/10.1083/jcb .201212038
- Linkert, M., C.T. Rueden, C. Allan, J.-M. Burel, W. Moore, A. Patterson, B. Loranger, J. Moore, C. Neves, D. Macdonald, et al. 2010. Metadata matters: Access to image data in the real world. *J. Cell Biol.* 189:777– 782. http://dx.doi.org/10.1083/jcb.201004104
- Lippincott, J., and R. Li. 1998. Sequential assembly of myosin II, an IQGAP-like protein, and filamentous actin to a ring structure involved in budding yeast cytokinesis. *J. Cell Biol.* 140:355–366. http://dx.doi.org/10.1083/jcb.140.2.355
- Longtine, M.S., A. McKenzie III, D.J. Demarini, N.G. Shah, A. Wach, A. Brachat, P. Philippsen, and J.R. Pringle. 1998. Additional modules for versatile and economical PCR-based gene deletion and modification in Saccharomyces cerevisiae. *Yeast.* 14:953–961. http://dx.doi.org/10.1002/(SICI)1097-0061(199807)14:10c953::AID-YEA293>3.0.CO;2-U
- McCusker, D., C. Denison, S. Anderson, T.A. Egelhofer, J.R.I. Yates III, S.P. Gygi, and D.R. Kellogg. 2007. Cdk1 coordinates cell-surface growth with the cell cycle. *Nat. Cell Biol.* 9:506–515. http://dx.doi.org/10.1038/ncb1568
- Nash, R., G. Tokiwa, S. Anand, K. Erickson, and A.B. Futcher. 1988. The WHI1+ gene of Saccharomyces cerevisiae tethers cell division to cell size and is a cyclin homolog. *EMBO J.* 7:4335–4346.
- Nurse, P. 1975. Genetic control of cell size at cell division in yeast. *Nature*. 256:547–551. http://dx.doi.org/10.1038/256547a0
- Pringle, J.R., A.E.M. Adams, D.G. Drubin, and B.K. Haarer. 1991. Immunofluorescence methods for yeast. *In Methods in Enzymology*. Cambridge, MA: Academic Press. 565–602.
- R Core Team. 2016. R: A language and environment for statistical computing.

 Available at https://www.gbif.org/tool/81287/r-a-language-and
 -environment-for-statistical-computing (Accessed September 15, 2017).
- RStudio Team. 2015. RStudio: Integrated Development Environment for R. Available at http://www.rstudio.com (Accessed September 15, 2017).
- Schmoller, K.M., J.J. Turner, M. Kõivomägi, and J.M. Skotheim. 2015. Dilution of the cell cycle inhibitor Whi5 controls budding-yeast cell size. *Nature*. 526:268–272. http://dx.doi.org/10.1038/nature14908
- Schneider, C.A., W.S. Rasband, and K.W. Eliceiri. 2012. NIH Image to ImageJ: 25 years of image analysis. *Nat. Methods*. 9:671–675. http://dx.doi.org/10.1038/nmeth.2089
- Thévenaz, P., U.E. Ruttimann, and M. Unser. 1998. A pyramid approach to subpixel registration based on intensity. *IEEE Trans. Image Process*. 7:27–41. http://dx.doi.org/10.1109/83.650848
- Wickham, H. 2009. ggplot2: Elegant Graphics for Data Analysis. New York: Springer-Verlag.
- Winey, M., and E.T. O'Toole. 2001. The spindle cycle in budding yeast. Nat. Cell Biol. 3:E23–E27. http://dx.doi.org/10.1038/35050663
- Wood, E., and P. Nurse. 2013. Pom1 and cell size homeostasis in fission yeast. *Cell Cycle*. 12:3228–3236. http://dx.doi.org/10.4161/cc.26462
- Young, P.G., and P.A. Fantes. 1987. Schizosaccharomyces pombe mutants affected in their division response to starvation. J. Cell Sci. 88:295–304.
- Zapata, J., N. Dephoure, T. Macdonough, Y. Yu, E.J. Parnell, M. Mooring, S.P. Gygi, D.J. Stillman, and D.R. Kellogg. 2014. PP2ARts1 is a master regulator of pathways that control cell size. *J. Cell Biol.* 204:359–376. http://dx.doi.org/10.1083/jcb.201309119